Available online at www.sciencedirect.com
ScienceDirect
Journal of the European Ceramic Society 28 (2008) 2521–2527
www.elsevier.com/locate/jeurceramsoc

Characterization and performance of glass–ceramic sealant to join metallic interconnects to YSZ and anode-supported-electrolyte in planar SOFCs

F. Smeacetto [a,*], M. Salvo [a], M. Ferraris [a], V. Casalegno [a], P. Asinari [b], A. Chrysanthou [c]

[a] *Department of Materials Science and Chemical Engineering, Politecnico di Torino, Corso Duca degli Abruzzi 24, 10129 Torino, Italy*
[b] *Department of Energetics, Corso Duca degli Abruzzi 24, 10129 Turin, Italy*
[c] *School of Aerospace, Automotive and Design Engineering, University of Hertfordshire, College Lane, Hatfield, Herts AL10 9AB, UK*

Received 22 December 2007; received in revised form 13 March 2008; accepted 20 March 2008
Available online 19 May 2008

Abstract

This work describes the design, development and performance of a glass–ceramic sealant used to join the ceramic electrolyte (YSZ wafer and anode-supported-electrolyte (ASE)) to the metallic interconnects (Crofer22 APU and AISI 430) in planar SOFC stacks. The designed glass–ceramic sealant is a barium-free silica-based glass, which crystallizes by means of the heat treatment after being deposited on substrates by the slurry technique.

The sealing process of the glass–ceramic was optimized and joined ceramic/seal/metal samples were morphologically characterized and tested for 400 h in air atmosphere followed by 200 h in H_2–3H_2O atmosphere at the fuel-cell operating temperature of 800 °C. The study showed that the use of the glass–ceramic was successful in joining the ceramic electrolyte to the metallic interconnect and in preventing adverse corrosion effects at the interface.

Keywords: Glass–ceramic; Fuel cell; Joining; Sealant; Interconnect

1. Introduction

Solid oxide fuel cells (SOFCs) are highly efficient energy conversion devices which produce electricity by the electrochemical reaction between fuel and an oxidant.[1–3] Among the different types of SOFCs, the planar type is expected to be cost-effective and mechanically robust and offers an attractive potential for increased power densities compared to other concepts.[4] A fuel-cell device is composed of an anode electrode (exposed to the fuel), an electrolyte and a cathode electrode (exposed to the oxidant).[5]

Several individual cells are connected in series in order to form a "stack" to obtain usable cell voltage and power. In a conventional SOFC, a dense yttria-stabilized zirconia (YSZ) oxygen-ion conducting electrolyte membrane separates a porous nickel–zirconia cermet anode and a doped lanthanum–manganite–perovskite cathode. The repeating unit of a planar configuration is formed by the combination of joint anode–electrolyte–cathode structures and interconnect which provides electrical connection between the anode of one individual cell (repeating unit) to the cathode of the neighbouring one.[6,7]

A key problem in the fabrication of planar SOFCs is the sealing of the electrolyte (yttria-stabilized zirconia wafer or anode-supported, depending on the cell configuration) with the metallic interconnect, in order to obtain a hermetic (gas tight) joint.

The materials selected as sealants must be thermo-mechanically and thermo-chemically stable in both oxidizing and wet-reducing environments at 800 °C for long-term exposures (500–1000 h).[8]

Currently, five main approaches are being studied for sealing SOFCs[8,9]: brazing[10], compressive seals[11,12], glass[13–16], glass–ceramic[17] and glass-composite seals.[18–21] Glasses and glass–ceramics show better resistance to the severe service environment (both oxidizing and reducing) than brazing alloys, and by carefully choosing the glass composition, they can meet most of the requirements that need to be exhibited by the ideal sealant material.[22–30]

Glass–ceramics can be prepared by controlled sintering and crystallization of glasses and have superior mechanical properties and higher viscosity at the SOFC operating temperature than

* Corresponding author. Tel.: +39 011564706; fax: +39 0115644699.
E-mail address: federico.smeacetto@polito.it (F. Smeacetto).

0955-2219/$ – see front matter © 2008 Elsevier Ltd. All rights reserved.
doi:10.1016/j.jeurceramsoc.2008.03.035

glasses. Furthermore, glass–ceramics can have thermal expansion coefficients very different from the parent glass, due to the different crystalline phases and their relative concentration. In order to develop a suitable glass–ceramic sealant, it is therefore necessary to understand the crystallization kinetics, the sealing properties and the chemical interactions when in contact with other components of the cell.[31,32] For example, barium aluminosilicate sealants have shown high reactivity with the metallic interconnect at 800–900 °C forming a porous and weak interface composed of barium chromate ($BaCrO_4$) and monocelsian ($BaAl_2Si_2O_8$)[33,34], while phosphate and borate glasses are not sufficiently stable in a humidified fuel gas environment.[35]

In a previous study, a barium- and boron-free glass–ceramic (labeled as SACN) was chosen to join Crofer22 APU alloy to an yttria-stabilized zirconia wafer. In the work that is reported here, the same glass–ceramic has been used to seal AISI 430 to YSZ and Crofer22 APU to the anode-supported-electrolyte (ASE) in order to examine the compatibility of the SACN composition with the metallic interconnect and the electrolyte. In addition, the joined samples were submitted to thermal ageing tests for 400 h in air atmosphere and, successively, for 200 h in H_2–$3H_2O$ atmosphere at the fuel-cell operating temperature of 800 °C. This paper describes the interaction of the sealant (SACN) with Crofer22 APU, AISI 430, YSZ and the anode-supported-electrolyte at 800 °C, at both reducing and oxidizing conditions.[36–38]

2. Experimental

The heat resistant metal alloys used for this study were Crofer22 APU (manufactured by ThyssenKrupp, Germany and supplied by HT Ceramix, Switzerland) and AISI 430 which are ferritic stainless steels containing 22 wt% and 16 wt% chromium, respectively, and exhibiting a thermal expansion coefficient of 11.2–11.5 × 10^{-6} K^{-1}. The Crofer22 APU was pre-oxidized as described in Ref. 1. The yttria 8 mol% zirconia wafer (with a thermal expansion coefficient of 10.5 × 10^{-6} K^{-1}) had a thickness of 200 μm. The anode-supported-electrolyte and the YSZ were supplied by HT Ceramix (Switzerland). The Crofer22 APU, AISI 430, YSZ, and ASE samples to be joined were cut to dimensions: 8 mm × 6 mm × 2 mm.

The sealant composition ranged between 53 and 58 mol% SiO_2, 6 and 8 mol% Al_2O_3, 24 and 26 mol% CaO, and 10 and 12 mol% Na_2O. The melting procedure, thermal and thermo-mechanical characterization of the sealant are described elsewhere.[1]

The T_g was found to be at 670 °C, $T_{softening}$ at 740 °C and two crystallization temperatures were detected (from DTA analysis) at 830 °C and 940 °C, respectively. Two crystalline phases were detected by XRD measurement in the glass–ceramic: $Ca_2Al_2SiO_7$ and $NaAlSiO_4$.

Studies of the wettability of the SACN glass on the AISI 430 alloy (as-received and preoxidised at 900 °C in air for 2 h) and on the ASE wafer were carried out by heating microscopy (LEITZ WETZLAR, Germany) or in a tubular oven under air or Ar atmosphere. The SACN glass powders (38–75 μm) were deposited on AISI 430 and ASE samples by slurry coating and heated to obtain the joint and subsequently examined by optical microscopy and scanning electron microscopy (SEM).

The slurry was made of a mixture of glass powder (38 < μm < 75) dispersed in ethanol (solid content 40 wt%).

The joined samples were obtained by placing the Crofer22 APU or AISI 430 plates on YSZ or YSZ surface of the anode-supported-electrolyte with the SACN slurry sandwiched in between. Heat treatments were performed in a tubular oven (Ar atmosphere) at a temperature above the glass softening point, without applying any load. Reproducible results, in terms of joint thickness and homogeneity were obtained. The joining thermal treatment was carried out from room temperature to 900 °C with a dwelling time of 30 min at 900 °C and a heating rate of 5 °C/min.

In order to evaluate the bonding strength of the glass–ceramic sealant, SACN and Crofer22 APU (about 6 mm × 6 mm) square samples were joined by the glass–ceramic to obtain a sandwich-like structure. A modification of ASTM C633-01[39] was designed and performed according to the apparatus reported in Fig. 1a, where the specimen is joined to the upper and lower grips by an epoxy resin (araldite AV 119). The Crofer22 APU/SACN/Crofer22 APU and AISI 430/SACN/AISI 430 joints were tested in uni-axial tension at room temperature, by using a loading rate of 0.5 mm/min.

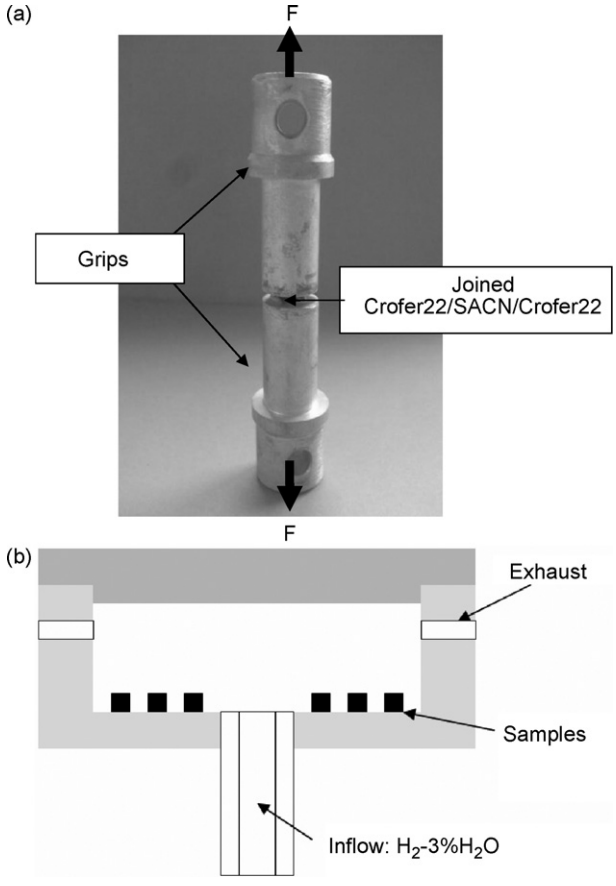

Fig. 1. (a) Experimental apparatus to measure the tensile strength of joints (Crofer22 APU/SACN/Crofer22 APU and AISI 430/SACN/AISI 430). (b) Experimental apparatus for exposure of joined samples to H_2–3%H_2O atmosphere at 800 °C.

Joined AISI 430/SACN/YSZ and Crofer22 APU/SACN/YSZ samples were submitted to thermal ageing in air atmosphere at 800 °C up to 400 h in a tubular furnace and, successively, exposed to H_2–3H_2O atmosphere (800 °C for 200 h). The experimental apparatus built for the tests consisted of an alumina cylinder (80 mm × 30 mm) containing the joined samples; this housing was connected to an alumina tube (diameter 10 mm) (see Fig. 1b) and filled with H_2–3%H_2O gas (500 N ml/min). The reducing mixture (H_2–3%H_2O) was obtained by using H_2 gas, which was humidified by passing over a water bath kept at a constant temperature of 22.8 °C.

The whole system was placed inside a furnace and a thermocouple was positioned near the samples in order to monitor the sample temperature. The heating rate was 30 °C/h and the dwelling time at 800 °C was 200 h.

Cross-sections of joined samples were characterized by SEM (FEI Inspect and Philips 525M) after polishing. EDS (SW9100 EDAX) analysis was carried out in order to detect any elemental diffusion into the seal before and after H_2–3%H_2O atmosphere exposure (800 °C for 200 h) and to study the chemical interactions of Crofer22 APU, AISI 430, and ASE with SACN at the three-phase-boundary at 800 °C under reducing and oxidizing conditions.

3. Results and discussion

3.1. Crofer22 APU/SACN/ ASE joined samples: morphological analysis

Fig. 2 shows a SEM micrograph of a Crofer22 APU/SACN/ASE cross-section. The joint region has an average thickness of 150/200 μm. Examination around the seal shows that a very low amount porosity (which is closed) is present, indicating that this sealant will provide high gas tightness and a hermetic structure. A very good adhesion between the glass–ceramic and both Crofer22 APU and YSZ can be observed. The choice of the glass–ceramic composition is partly based on the value of its thermal expansion coefficient of $10.7 \times 10^{-6}\,K^{-1}$ [1] which matches very well those of Crofer22 ($11.2–11.5 \times 10^{-6}\,K^{-1}$) and YSZ ($10.5 \times 10^{-6}\,K^{-1}$). The absence of cracks near the interface of the glass–ceramic with both Crofer22 APU and YSZ demonstrates their good physical compatibility with the SACN glass–ceramic. Fig. 3 is a magnification (rectangular area in Fig. 2) of the interface zone between the glass–ceramic and the YSZ. The interface is continuous and without pores or cracks. Two distinct zones can be observed in the anode-supported-electrolyte; the upper zone in the figure represents the porous anode, while the lower region shows the dense YSZ electrolyte. The thickness of the YSZ electrolyte, supported on the anode, is about 5 μm. This feature ensures the capability of the SOFC to operate at a temperature of 800 °C.

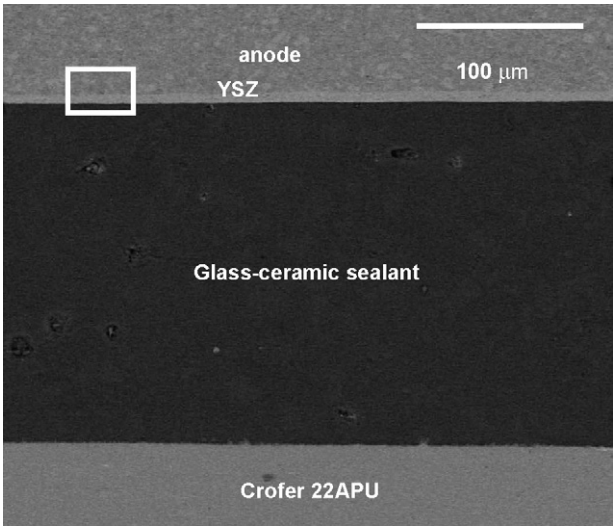

Fig. 2. Crofer22 APU/SACN/ASE SEM cross-section.

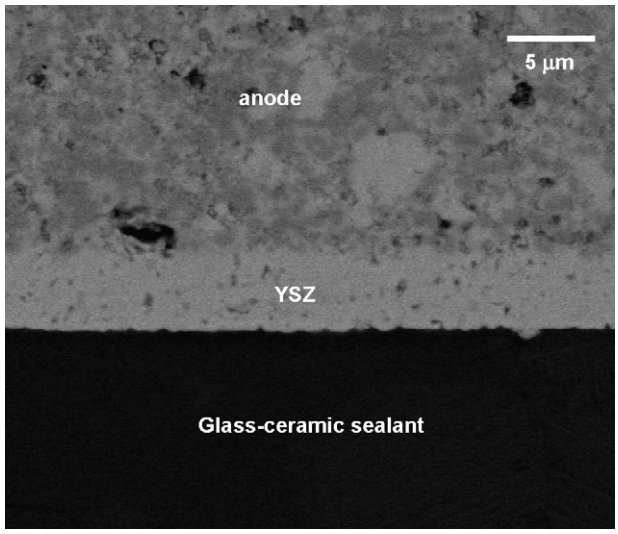

Fig. 3. SEM cross-section of the interface zone between the SACN and the YSZ side of ASE in Crofer22 APU/SACN/ASE joined sample.

3.2. AISI 430/SACN/YSZ joined samples: morphological analysis

A SEM cross-section image of the AISI 430/SACN/YSZ joined sample is shown in Fig. 4a. Both interfaces are continuous and defect-free. The SACN adhered well to both the preoxidised AISI 430 and YSZ substrates. Concerning the AISI 430/SACN interface, it must be highlighted that in order to obtain a good adhesion between AISI 430 and the glass–ceramic sealant, the preoxidation heat-treatment (900 °C, 2 h, air) was essential, since in the case of the as-received AISI 430, the glass–ceramic layer was detached from the metallic interconnect. The pre-oxidation treatment gave rise to the formation of a 1–2 μm thick chromium–manganese–iron oxide layer, as detected by means of XRD.

Fig. 4b shows the SEM micrograph of the AISI 430/SACN interface. The coherent pre-oxidation layer is clearly visible. The SACN glass–ceramic adhered well to the preoxidised AISI 430 and a defect-free structure, without voids and micro-cracks, can be observed.

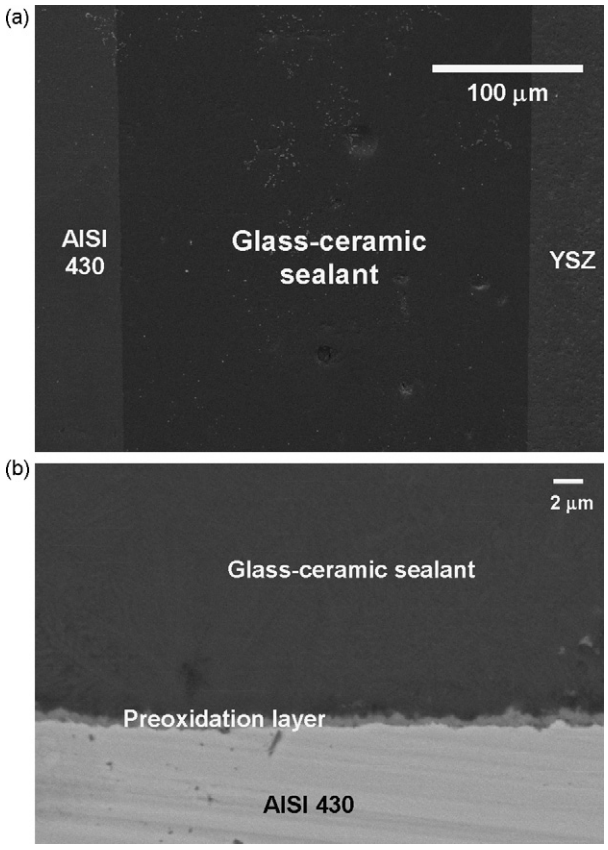

Fig. 4. (a) AISI 430/SACN/YSZ SEM cross-section and (b) AISI 430/SACN interface: SEM cross-section.

3.3. Crofer22 APU/SACN/YSZ joined sample exposure to H_2–3%H_2O atmosphere

The Crofer22 APU/SACN/YSZ joined samples were previously tested in air at 800 °C up to 400 h. The results of the thermal ageing are reported in detail in a previous paper.[1]

After a mid-term exposure (200 h) at 800 °C in a reducing atmosphere (H_2–3%H_2O), it was observed that the seal remained intact. Fig. 5 shows a SEM cross-section of the of Crofer22 APU/SACN/YSZ sample after 200 h exposure to H_2–3%H_2O atmosphere. The SEM micrograph is focused on the central part of the joined sample. It is evident that no interfacial delamination at the glass–ceramic/steel interface took place. It can be also observed that the joint region does not exhibit substantial modifications from the morphological point of view. No cracks or pores are present, and the interfaces between the SACN glass–ceramic and both Crofer22 APU alloy and YSZ ceramic are still continuous and free of cracks.

As described before, the Crofer22 APU was preoxidised (900 °C, 2 h) before the joining process. It has previously been reported[15] that the oxidation of Crofer22 APU in air resulted in a chromium–manganese oxide layer at the alloy surface. The oxide layer is thermodynamically very stable. Fig. 5a shows a detail of the interface between the SACN glass–ceramic and the pre-oxidized Crofer22 APU, where the chromium–manganese oxide layer is clearly visible. EDS spot-analysis conducted at point 1 revealed the presence of chromium, manganese

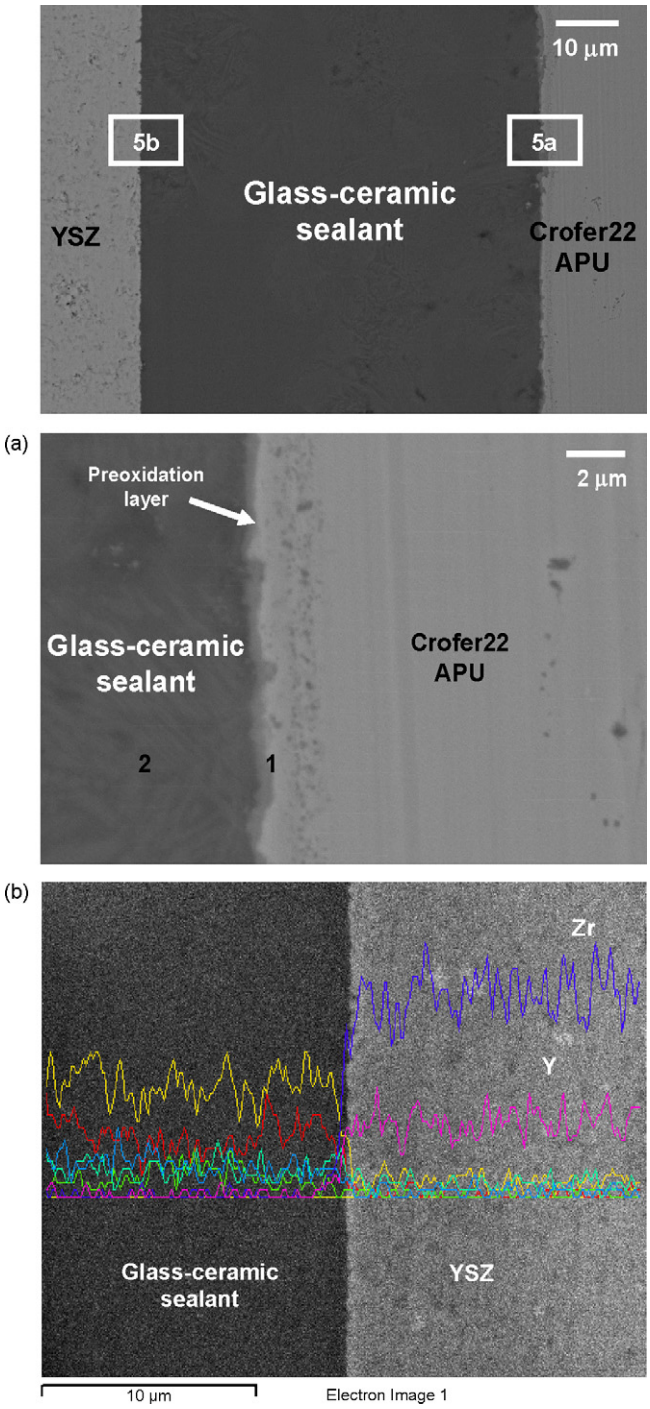

Fig. 5. Crofer22 APU/SACN/YSZ after exposure to H_2–3%H_2O atmosphere at 800 °C up to 200 h: SEM cross-section, (a) Crofer22 APU/SACN interface after exposure to H_2–3%H_2O atmosphere at 800 °C up to 200 h and (b) YSZ/SACN interface after exposure to H_2–3%H_2O atmosphere at 800 °C up to 200 h.

and oxygen, while at point 2 only O, Na, Al, Si and Ca were detected (as before exposure to H_2–3%H_2O atmosphere). This observation confirmed that no undesired reactions took place and no corrosion products were formed at the Crofer22 APU-glass–ceramic sealant interface during exposure to the H_2–3%H_2O atmosphere. As discussed by Ogasawara et al.[40], the enrichment of sodium in the pre-oxidation layer is potentially dangerous and can lead to the formation of Na_2CrO_4. The

high vapour pressure of this alkali chromate can result in its vaporization which can be accompanied by the decomposition and removal of the $(Mn,Cr)_3O_4$ spinel oxide, and chromium depletion in the surface vicinity. In addition, depletion of sodium from the SACN at the interface with Crofer22 APU is likely to reduce the quality of the joint due to the formation of cracks. Interfacial delamination cracks between the sealant and the metallic interconnect must be avoided, because they can act as a preferential path for fuel transport.

In contrast to the study by Ogasawara et al.[40], the results of the present study showed that there was no transport of sodium away from the SACN sealant which maintained good adhesion to the two substrates. The reason for this was probably due to the higher thermodynamic stability of the SACN glass–ceramic that was used in the present study compared to the glass sealant used by Ogasawara et al.[40]. The main composition difference between the two studies was that the glass ceramic that was used in the present study contained 20–23% CaO, while the glass sealant used in Ref. 40 had no CaO at all. Unfortunately Ogasawara et al.[40] provided only the composition of the glass sealant that they used, but gave no information on the phases that were present. As a result a thermodynamic comparison between the two sealants is not possible. However, the high amount of CaO in the glass–ceramic used in the present study is very likely to lead to the formation of a more stable oxide at the interface.

Fig. 5b shows a magnification of the interface between the SACN glass–ceramic and YSZ indicating that the interface is free of pores and cracks. An EDS line scan analysis (from YSZ to 15 μm into the glass–ceramic; Fig. 5b) revealed no diffusion of yttrium from YSZ into the glass–ceramic. This result confirmed the thermo-chemical compatibility of the SACN and YSZ at 800 °C under a dual atmosphere. This is in contrast with what was previously observed by Lahl et al.[31], where the presence of CaO in glasses in contact with YSZ lead to the formation of monoclinic ZrO_2, because of yttrium diffusion into glass. This result could be detrimental to SOFCs, because of the formation of monoclinic ZrO_2 could lead to the formation of cracks at the interface.

Since corrosion products and undesired reactions between the glass–ceramic and Crofer22 APU could be found at the three-boundary zone (metal–sealant–gas)[41] after exposure to reducing conditions for 200 h, SEM was conducted at the edges of the joined samples.

Fig. 6 shows a magnification of the three-phase-boundary zone, between Crofer22 APU, the glass–ceramic and the H_2–3%H_2O atmosphere at 800 °C after 200 h at 800 °C. A grain boundary-dominated internal oxidation in Crofer22 APU (corrosion zone) can be observed only in the area that is not protected by the SACN glass–ceramic sealant. In our system (SACN/Crofer22 APU), there was no internal oxidation of the ferritic steel beneath the SACN glass–ceramic sealant and the quality of the bond between the SACN and Crofer22 APU was still outstanding. The crystalline phases of the SACN glass–ceramic did not change after thermal ageing, thus confirming the thermo-chemical stability of the SACN glass–ceramic seal.

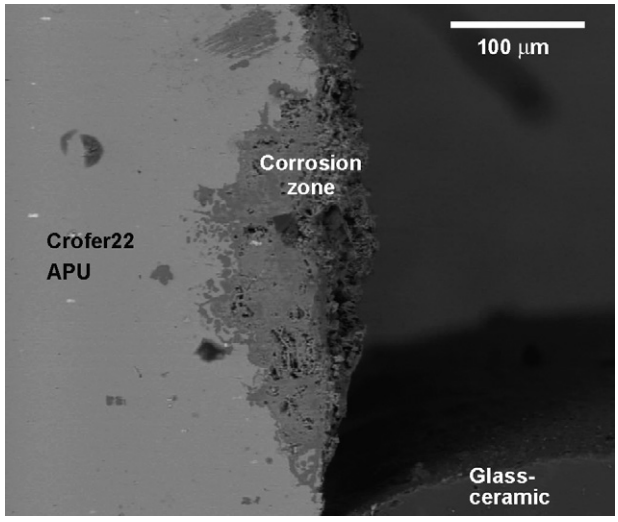

Fig. 6. Magnification of the three-phase-boundary zone, between Crofer22 APU, SACN and H_2–3%H_2O atmosphere at 800 °C, 200 h (Crofer22 APU/SACN/YSZ joint).

3.4. AISI 430/SACN/YSZ joined samples exposure to air and H_2–3%H_2O atmospheres

These joined samples were first subjected to heat-treatment in air for up to 400 h at 800 °C. Examination of a cross-section of the joint sample indicated that there were no cracks near the interface. As for the Crofer22 APU/SACN/YSZ system, SEM and XRD observations in the AISI 430/SACN/YSZ joint confirmed that no undesirable reactions took place and no corrosion products were formed at the AISI 430-glass–ceramic sealant interface.

Concerning the AISI 430/SACN/YSZ samples exposed to H_2–3%H_2O atmosphere, as for the Crofer22 APU/SACN/YSZ system, there was no formation and vaporization of alkali chromates and consequently there was no chromium depletion at the three-phase-boundary. As a consequence, no swelling of the metal with consequent bulging was observed. Fig. 7 shows a SEM cross-section of an AISI 430/SACN/YSZ sample; it can be observed that no interfacial delaminations at the glass–ceramic steel interface took place. Fig. 7b presents a magnification of AISI 430/SACN interface; also in this case no undesired reactions took place and no corrosion products were formed at the interface, as confirmed by EDS analyses. Fig. 7c shows the AISI 430/SACN interface at the three-phase-boundary after the tests in H_2–3%H_2O atmospheres. As discussed for the Crofer22 APU/SACN samples, there was no internal oxidation within the zones where the SACN covered the metal alloy.

3.5. Bonding strength of Crofer22 APU to glass–ceramic sealant

The bond strength of the joint between the Crofer22 APU and the glass–ceramic was investigated by carrying out uniaxial tensile tests at room temperature.[42] The average tensile

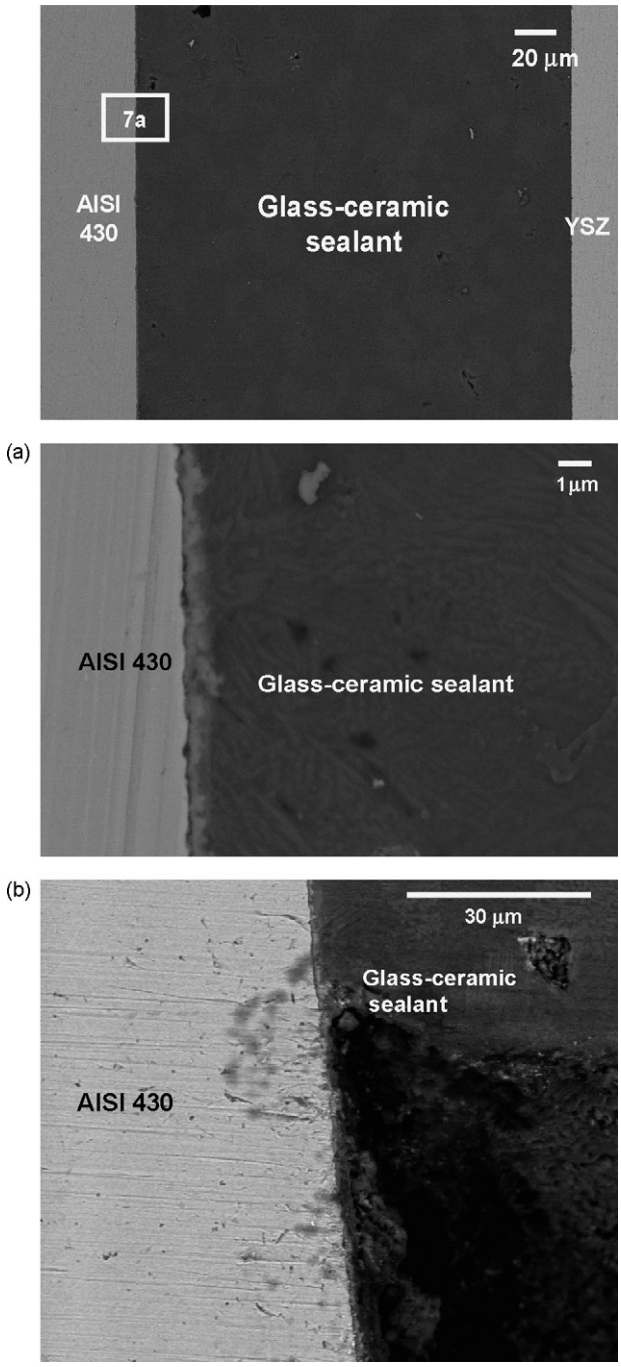

Fig. 7. SEM cross-section of the of pre-oxidized AISI 430/SACN/YSZ sample after exposure to H_2–3%H_2O atmosphere at 800 °C up to 200 h. (a) SEM magnification of pre-oxidized AISI 430/SACN interface after exposure to H_2–3%H_2O atmosphere at 800 °C up to 200 h and (b) magnification of the three-phase-boundary zone, between pre-oxidized AISI 430, SACN and H_2–3%H_2O atmosphere at 800 °C up to 200 h.

strength value was 6 MPa. Fig. 8 shows the fracture surfaces where 2 layers of SACN are viewable on both Crofer22 APU samples. Examination of these samples revealed that the fracture always occurred through the glass–ceramic and never at the metallic interconnect/glass–ceramic interface. This observation suggested that the bonding strength for the joint was high with very good adhesion.

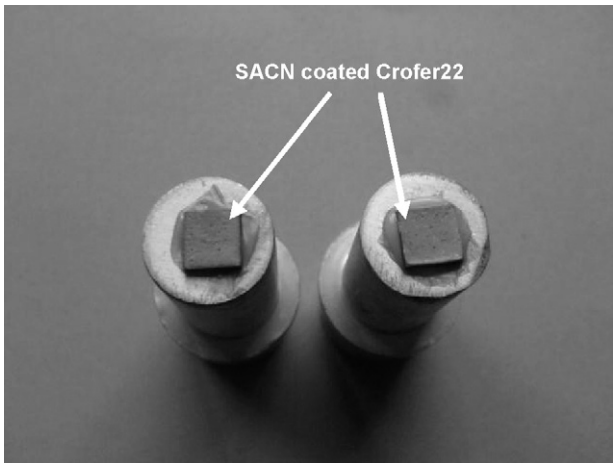

Fig. 8. Fracture surfaces of Crofer22 APU/SACN.

4. Conclusions

A detailed characterization and performance of a glass–ceramic sealant that was specially developed for use in SOFCs to join the metallic interconnects Crofer22 APU and AISI 430 to the YSZ and anode-supported-electrolyte, was carried out. The tests of the joined samples after exposure to air and humidified hydrogen at 800 °C (respectively for 400 and 200 h) revealed no corrosion products at the interfaces between metallic interconnects and glass–ceramic sealant. There was no chromium depletion at the surface of the Crofer22 APU close to the three-phase-boundary. As a consequence, no swelling of the metal (both Crofer22 APU and AISI 430) with subsequent bulging was observed. The overall conclusion of the work that was presented was that the glass–ceramic sealant was effective to joining both Crofer22 APU and anode-supported-electrolyte.

Acknowledgments

The authors gratefully acknowledge the help of HTCeramix who supplied the Crofer22 APU interconnect and electrolyte materials for the study. The contribution of Ms Alexandra Copado (student from INSA de Lyon, France) during her visit at Politecnico di Torino is also acknowledged. Thanks are also extended to Paolo Squillari (Energetics Department, Politecnico di Torino) for his important assistance in conducting the humidified hydrogen atmosphere tests.

This work was supported in part by the EU Network of Excellence project in "Knowledge-based Multicomponent Materials for Durable and Safe Performance" (KMM-NoE) under contract no. NMP3-CT-2004-502243.

References

1. Smeacetto, F., Salvo, M., Ferraris, M., Cho, J. and Boccaccini, A. R., Glass–ceramic seal to join Crofer 22 APU alloy to YSZ ceramic in planar SOFCs. *J. Eur. Ceram. Soc.*, 2008, **28**, 61–68.
2. Steele, B. C. H. and Heinzel, A., *Mater. Fuel Cell Technol. Nat.*, 2001, **414**, 345–352.
3. Singh, R. N., Sealing technology for solid oxide fuel cells (SOFC). *Int. J. Appl. Ceram. Technol.*, 2007, **4**, 134–144.

4. Wen, T.-L., Wang, D., Chen, M., Tu, H., Lu, Z., Zhang, Z., Nie, H. and Huang, W., Material research for planar SOFC stack. *Solid State Ionics*, 2002, **148**, 13–519.
5. Haile, S. M., Fuel cell materials components. *Acta Mater.*, 2003, **51**, 5981–6000.
6. Zhu, W. Z. and Deevi, S. C., Development of interconnect materials for solid oxide fuel cells. *Mater. Sci. Eng. A*, 2003, **348**, 227–243.
7. Antepara, I., Villarreal, I., Rodrıguez-Martınez, L. M., Lecanda, N., Castro, U. and Laresgoiti, A., Evaluation of ferritic steels for use as interconnects and porous metal supports in IT-SOFCs. *J. Power Sources*, 2005, **151**, 103–107.
8. Fergus, J. W., Sealants for solid oxide fuel cells. *J. Power Sources*, 2005, **147**, 46–57.
9. Weil, K. S., The state-of-the-art in sealing technology for solid oxide fuel cells. *JOM*, August 2006, 36–44.
10. Singh, M., Shpargel, T. P. and Asthana, R., Brazing of stainless steel to yttria-stabilized zirconia using gold-based brazes for solid oxide fuel cell applications. *Int. J. Appl. Ceram. Technol.*, 2007, **4**, 119–133.
11. Le, S., Sun, K., Zhang, N., Shao, Y., An, M., Fu, Q. and Zhu, X., Comparison of infiltrated ceramic fiber paper and mica base compressive seals for planar solid oxide fuel cells. *J. Power Sources*, 2007, **168**, 447–452.
12. Wiener, F., Bram, M., Buchkremer, H. P. and Sebold, D., Chemical interaction between Crofer 22 APU and mica-based gaskets under simulated SOFC conditions. *J. Mater. Sci.*, 2007, **42**, 2643–2651.
13. Bansal, N. P. and Gamble, E. A., Crystallization kinetics of a solid oxide fuel cell seal glass by differential thermal analysis. *J. Power Sources*, 2005, **47**, 107–115.
14. Chou, Y.-S., Stevenson, J. and Gow, R. N., Novel alkaline earth silicate sealing glass for SOFC. Part I. The effect of nickel oxide on the thermal and mechanical properties. *J. Power Sources*, 2007, **168**, 426–433.
15. Chou, Y.-S., Stevenson, J. and Gow, R. N., Novel alkaline earth silicate sealing glass for SOFC. Part II. Sealing and interfacial microstructure. *J. Power Sources*, 2007, **170**, 395–400.
16. Lara, C., Pascual, M. J. and Duran, A., Glass-forming ability, sinterability and thermal properties in the systems RO–BaO–SiO_2 (R = Mg, Zn). *J. Non-Cryst. Solids*, 2004, **348**, 149–155.
17. Goel, A., Tulyaganov, D. U., Agathopoulos, S., Ribeiro, M. J. and Ferreira, J. M. F., Crystallization behaviour, structure and properties of sintered glasses in the diopside-Ca-Tschermak system. *J. Eur. Ceram. Soc.*, 2007, **27**, 3231–3238.
18. Brochu, M., Gauntt, B. D., Shah, R. and Loehman, R. E., Comparison between micrometer- and nano-scale glass composites for sealing solid oxide fuel cells. *J. Am. Ceram. Soc.*, 2006, **89**, 810–816.
19. Brochu, M., Gauntt, B. D., Shah, R., Miyake, G. and Loehman, R. E., Comparison between barium and strontium-glass composites for sealing SOFCs. *J. Eur. Ceram. Soc.*, 2006, **26**, 3307–3313.
20. Deng, X., Duquette, J. and Petric, A., Silver–glass composite for high temperature sealing. *Int. J. Appl. Ceram. Technol.*, 2007, **4**, 145–151.
21. Smeacetto, F., Salvo, M., Ferraris, M., Casalegno, V. and Asinari, P., Glass and composite seals for the joining of YSZ to metallic interconnect in solid oxide fuel cells. *J. Eur. Ceram. Soc.*, 2007, **28**(3), 611–616.
22. Flugel, A., Dolan, M. N., Varshneya, A. K., Zheng, Y., Coleman, N., Hall, M., Earl, D. and Misture, S. T., Development of an improved devitrifiable fuel cell sealing glass. *J. Electrochem. Soc.*, 2007, **154**(6), B601–B608.
23. Pascual, M. J., Guillet, A. and Duran, A., Optimization of glass–ceramic sealant compositions in the system MgO–BaO–SiO_2 for solid oxide fuel cells (SOFC). *J. Power Sources*, 2007, **169**, 40–46.
24. Wang, R., Liu, Z., Liu, C., Zhu, R., Huang, X., Wei, B., Ai, N. and Su, W., Characteristics of a SiO_2–B_2O_3–Al_2O_3–BaO–PbO_2–ZnO glass–ceramic sealant for SOFCs. *J. Alloys Compd.*, 2007, **432**(1–2), 189–193.
25. Gosh, S., Kundu, P., Das Sharma, A., Basu, R. N. and Maiti, H. S., Microstructure and property evaluation of barium aluminosilicate glass–ceramic sealant for anode-supported solid oxide fuel cell. *J. Eur. Ceram. Soc.*, 2008, **28**, 69–76.
26. Steinberger, R., Blum, L., Buchkremer, H. P., Gross, S., De Haart, L., Hilpert, K., Nabielek, H., Quadakkers, W., Reisgen, U., Steinbrech, R. W. and Tietz, F., *Int. J. Appl. Ceram. Technol.*, 2006, **3**, 470–476.
27. Lara, C., Pascual, M. J., Keding, R. and Duran, A., Electrical behaviour of glass–ceramics in the systems RO-BaO-SiO_2 (R = Mg, Zn) for sealing SOFCs. *J. Power Sources*, 2006, **157**, 377–384.
28. Pascual, M. J., Kharton, V. V., Tsipis, E., Yaremchenko, A. A., Lara, C., Duran, A. and Frade, J. R., Transport properties of sealants for high-temperature electrochemical applications: RO–BaO–SiO_2 (R = Mg, Zn) glass–ceramics. *J. Eur. Ceram. Soc.*, 2006, **26**, 3315–3324.
29. Singh, R. N., High temperature seals for solid oxide fuel cells. *J. Mater. Eng. Perform.*, 2006, **15**, 422–426.
30. Malzbender, J., Monch, J., Steinbrech, R. W., Koppitz, T., Gross, S. M. and Remmel, J., Symmetric shear test of glass–ceramic sealants at SOFC operation temperature. *J. Mater. Sci.*, 2007, **42**, 6297–6301.
31. Lahl, N., Bahadur, D., Singh, K., Singheiser, L. and Hilpertz, K., Chemical interactions between aluminosilicate base sealants and the components on the anode side of solid oxide fuel cells. *J. Electrochem. Soc.*, 2002, **149**, A607–A614.
32. Bahadur, D., Lahl, N., Singh, K., Singheiser, L. and Hilpert, K., Influence of nucleating agents on the chemical interaction of MgO–Al_2O_3–SiO_2–B_2O_3 glass sealants with components of SOFCs. *J. Electrochem. Soc.*, 2004, **151**, A558–A562.
33. Batfalsky, P., Haanappel, V. A. C., Malzbender, J., Menzler, N. H., Shemet, V., Vinke, I. C. and Steinbrech, R. W., Chemical interaction between glass–ceramic sealants and interconnect steels in SOFC stacks. *J. Power Sources*, 2006, **155**, 128–137.
34. Yang, Z., Meinhardt, Kerry, D. and Stevenson, J. W., Chemical compatibility of barium–calcium–aluminosilicate-based sealing glasses with the ferritic stainless steel interconnect in SOFCs. *J. Electrochem. Soc.*, 2003, **150**, A1095–A1101.
35. Larsen, P. H., The influence of SiO_2 addition to 2MgO–Al_2O_3–3.3P_2O_5 glass. *J. Non-Cryst. Solids*, 1999, **244**, 16–24.
36. Haanappel, V. A. C., Shemet, V., Vinke, I. C., Gross, S. M., Koppitz, T., Menzler, N. H., Zahid, M. and Quadakkers, W. J., Evaluation of the suitability of various glass sealant-alloy combinations under SOFC stack conditions. *J. Mater. Sci.*, 2005, **40**, 1583–1592.
37. Nielsen, K. A., Solvang, M., Nielsen, S. B. L., Dinesen, A. R., Beeaff, D. and Larsen, P. H., Glass composite seal for SOFC application. *J. Eur. Ceram. Soc.*, 2007, **27**, 1817–1822.
38. Menzler, N. H., Sebold, D., Zahid, M., Gross, S. M. and Koppitz, T., Interaction of metallic SOFC interconnect materials with glass–ceramic sealant in various atmosphere. *J. Power Sources*, 2005, **152**, 156–167.
39. ASTM C633-01, *Standard Test Method for Adhesion or Cohesion Strength of Thermal Spray Coatings*, 2001.
40. Ogasawara, K., Kameda, H., Matsuzaki, Y., Sakurai, T., Uehara, T., Toji, A., Sakai, N., Yamaji, K., Horita, T. and Yokokawa, H., Chemical stability of ferritic alloy interconnect for SOFCs. *J. Electrochem. Soc.*, 2007, **154**(7), B657–B663.
41. Menzler, N. H., Sebold, D., Zahid, M., Gross, S. M. and Koppitz, T., Interaction of metallic SOFC interconnect materials with glass–ceramic sealant in various atmospheres. *J. Power Sources*, 2005, **152**, 156–167.
42. Chou, Y., Biskie, B. D., Stevenson, J. W. and Singh, P., *Effect of Pre-Oxidation of a Metallic Interconnect on the Bonding Strength of a SOFC Sealing Glass*, In Book of Abstracts 31st International Conference on Advanced Ceramics and Composites, Daytona Beach, FL, USA, January 21–26, 2007.